



Aalborg Universitet

AALBORG UNIVERSITY
DENMARK

Upgrading of Nondewatered Nondemetalized Lignocellulosic Biocrude from Hydrothermal Liquefaction Using Supercritical Carbon Dioxide

Montesantos, Nikos; Nielsen, Rudi P.; Maschietti, Marco

Published in:
Industrial & Engineering Chemistry Research

DOI (link to publication from Publisher):
[10.1021/acs.iecr.9b06889](https://doi.org/10.1021/acs.iecr.9b06889)

Publication date:
2020

Document Version
Accepted author manuscript, peer reviewed version

[Link to publication from Aalborg University](#)

Citation for published version (APA):
Montesantos, N., Nielsen, R. P., & Maschietti, M. (2020). Upgrading of Nondewatered Nondemetalized Lignocellulosic Biocrude from Hydrothermal Liquefaction Using Supercritical Carbon Dioxide. *Industrial & Engineering Chemistry Research*, 59(13), 6141-6153. <https://doi.org/10.1021/acs.iecr.9b06889>

General rights

Copyright and moral rights for the publications made accessible in the public portal are retained by the authors and/or other copyright owners and it is a condition of accessing publications that users recognise and abide by the legal requirements associated with these rights.

- Users may download and print one copy of any publication from the public portal for the purpose of private study or research.
- You may not further distribute the material or use it for any profit-making activity or commercial gain
- You may freely distribute the URL identifying the publication in the public portal -

Take down policy

If you believe that this document breaches copyright please contact us at vbn@aub.aau.dk providing details, and we will remove access to the work immediately and investigate your claim.

1 Upgrading of non-dewatered non-demetalized lignocellulosic bio-crude from
2 hydrothermal liquefaction using supercritical carbon dioxide

3 Nikolaos Montesantos, Rudi P. Nielsen, Marco Maschietti*

4 Department of Chemistry and Bioscience, Aalborg University, Niels Bohrs Vej 8A, 6700, Esbjerg,
5 Denmark

6 * E-mail: marco@bio.aau.dk

7 Abstract

8 Supercritical carbon dioxide (sCO₂) extraction was applied on a raw bio-crude, obtained by
9 hydrothermal liquefaction of pinewood. The extractions were carried out in semicontinuous mode, in
10 the range 80 to 150 °C and 330 to 450 bar. Extraction yields from 44 to 53 wt% were achieved. The
11 extracts were richer in lower molecular weight (MW) compounds, with fatty acids and aromatic
12 hydrocarbons concentrated up to 14 and 24 wt%, respectively. For comparable MWs, lower polarity
13 compounds concentrated in the extracts. Compared to the feed, the extracts exhibited lower density
14 (from 1030 kg/m³ down to 914 kg/m³), lower water content (from 5.7 wt% down to 1.3 wt%) and
15 lower oxygen content (from 10.0 wt% down to 5.0 wt%). In addition, the metal content was drastically
16 reduced (from 8500 mg/kg down to 170 mg/kg on average). In the context of biofuel production, the
17 sCO₂ extracts are a better feed for catalytic hydrotreating.

18

19 1. Introduction

20 Hydrothermal liquefaction (HTL) is a promising thermochemical process to produce liquid fuel from
21 biomass. The process entails the depolymerisation of biomass in an aqueous medium at high
22 temperature (e.g. 250 – 450 °C) and pressure (e.g. 100 – 350 bar).¹ One of the major advantages of
23 HTL involves the flexibility of feedstocks that can be processed, which include both dry and wet
24 biomasses.² The utilization of lignocellulosic biomass, an example of so-called second generation
25 biomass, is particularly appealing due to lack of direct competition with food production. Wood residue
26 and excess lignin from the paper pulp industry are examples of lignocellulosic by-products produced in
27 large quantities, which can be valorised to liquid fuels via HTL.^{3–5}

28 Besides the water medium, the HTL process is typically carried out in the presence of homogeneous
29 catalysts and pH adjusters, such as potassium carbonate (K_2CO_3), sodium carbonate (Na_2CO_3), and
30 sodium hydroxide (NaOH).^{1,6} The main products of HTL are a CO_2 -rich gas phase (typically around 90
31 wt% CO_2),^{7,8} a solid phase (i.e. char) and two liquid phases. The liquid products are an aqueous phase
32 saturated of water-soluble organics and an oil, namely the HTL bio-crude.¹

33 The HTL bio-crude obtained by gravimetric separation of the products is a tight water-in-oil emulsion,
34 with water content in the range 5 to 15 wt%.^{9–12} Typical ash content values are reported broadly
35 ranging from 0.01 wt% up to 5 wt%.^{4,10,13} Individual values of the content of alkali and earth metals
36 (e.g. potassium and iron) are typically not reported, except for a few cases.^{3,4} In comparison to fossil
37 crude oils, HTL bio-crudes have relatively high oxygen content, typically in the range 10 to 20
38 wt%.^{10,12,14,15} The high oxygen content is caused by a variety of oxygenated components, such as
39 ketones, fatty acids and different one-ring phenols (e.g. phenol, guaiacols, catechols). Moreover,
40 oxygen is also expected to be contained in a complex large fraction of high boiling components,

41 including phenolic oligomers derived from the lignin fraction.¹⁶ The presence of a relatively large
42 heavy fraction, essentially non-volatile, is evident from previous works reporting vacuum distillation of
43 lignocellulosic HTL bio-crudes. It was observed that approximately 50 wt% of the oil cannot be
44 distilled even at very high vacuum (i.e. 1.3 mbar) at temperatures between 130 °C and 160 °C. The
45 atmospheric equivalent boiling point of this heavy fraction was above 400 °C.^{17,18} In the reported
46 distillation experiments, the bio-crude was dewatered prior the process, since the presence of water
47 would reduce the distillation efficiency, result to unsteady boiling and create control issues.¹⁷ In
48 addition to the above, HTL lignocellulosic bio-crudes have high viscosity (typically in the range 10^3 to
49 10^6 cP)¹⁹⁻²¹ and high density (typically above 1000 kg/m^3)^{5,7,20,22}.

50 In order to utilize HTL bio-crudes as drop-in biofuels, the oxygen content has to be drastically reduced.
51 The state of the art method for this purpose is catalytic hydrotreating (i.e. hydrodeoxygenation,
52 HDO).²³ However, hydrotreating of raw HTL bio-crudes can lead to accelerated deactivation of the
53 catalytic bed due to high metal content, which originates from the alkali catalysts used in the HTL
54 process and, to some extent, from the biomass itself.^{21,24} These metals deposit on the active sites of the
55 catalyst and promote sintering during catalyst regeneration.²⁵ Both of these mechanisms are
56 irreversible. Even at low concentrations, metals can drastically reduce the lifetime of the catalyst,
57 which needs to be replaced when the deposition of 3 – 4 wt% of metals is reached.²⁶ In addition, water
58 can reduce catalyst activity by modifying its surface or the pore structure.²⁵ Less water and oxygen in
59 the HDO feed is therefore beneficial due to the lower hydrogen requirement of the process and the
60 lower amount of water in the HDO reactor. In addition, reduced density values for the bio-crude are
61 desirable in order to increase the drop-in potential with different types of petroleum fuels, such as
62 kerosene (775 to 840 kg/m^3),²⁷ diesel (820 to 845 kg/m^3)²⁸ and marine fuels (up to 991 kg/m^3).²⁹

63 The application of a separation process upstream the hydrotreating, aimed at obtaining a large fraction
64 of HTL bio-crude exhibiting favourable properties for the hydrotreating process itself (especially low
65 water, oxygen and metal content), is worth analysing. Among alternative separation processes,
66 supercritical carbon dioxide (sCO₂) extraction is appealing for a number of reasons: i) it is an
67 environmentally friendly process, thus suitable by nature for the sustainability paradigm that should
68 characterize biofuel production; ii) CO₂ is internally generated in the HTL process; iii) it is a process
69 competitive to distillation in the presence of high boiling point oils, as temperatures required in
70 distillation may be too high even at high vacuum.³⁰ The separation of high boiling point liquid mixtures
71 using sCO₂ is at industrial level for the fractionation of perfluoropolyether oligomers³¹ and it has been
72 applied at pilot or demonstration scale in a number of cases. Some representative examples include the
73 separation of fish oil ethyl esters,^{32,33} or the removal of fatty acids from rice bran oil,³⁴ wheat germ oil³⁵
74 and olive oil deodorizer distillate.³⁶

75 In previous works, sCO₂ was reported capable of extracting a large fraction of a dewatered and
76 demetalized lignocellulosic bio-crude (extraction yields up to 49 wt%).^{22,37} The procedure used for the
77 dewatering and demetalization of the bio-crude used in the mentioned previous works^{22,37} is based on
78 dilution of the bio-crude in methyl ethyl ketone followed by washing in citric acid aqueous solutions.
79 Details on the procedure are available in the PhD Thesis of Jensen.³⁸ The previous works^{22,37}
80 demonstrated problem-free operation above 80 °C (i.e. 80 – 120 °C), while the extractions were not
81 smooth and sometimes characterized by equipment clogging at 40 °C and 60 °C. The only other works
82 found on extraction of lignocellulosic bio-crudes refer to pyrolysis oils, where the extracts
83 demonstrated lower viscosity,³⁹ and lower water content than the corresponding feeds.^{40,41}

84 The aim of this work is to assess the sCO₂ extraction process on a raw HTL bio-crude, which is to say a
85 non-dewatered non-demetalized bio-crude obtained by gravimetric separation downstream the HTL
86 reactor and without any further treatment. The specific objective of this work is therefore to assess the
87 potential of sCO₂ extraction in carrying out dewatering, demetalization and bio-crude separation in a
88 single process step, as well as to compare the characteristics of the sCO₂ separation on this raw bio-
89 crude with the separation reported in previous works referring to a dewatered and demetalized bio-
90 crude^{22,37}. In addition, the tested operating conditions were expanded to higher pressures (up to 450
91 bar) and temperatures (up to 150 °C), as the previous works^{22,37} indicated a positive effect with
92 increasing these parameters. Extraction temperatures below 80 °C were instead not considered, due to
93 the above-mentioned operating problems.

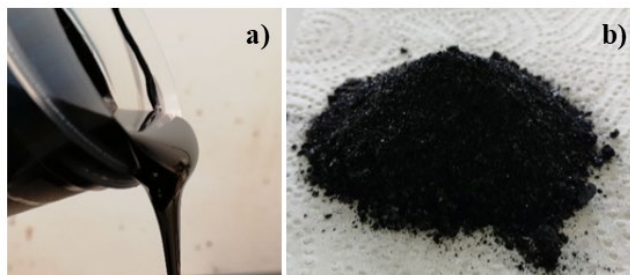
94 2. Materials and methods

95 2.1. Materials

96 2.1.1. Feed bio-crude

97 The feed HTL bio-crude was produced by continuous-flow hydrothermal liquefaction of pinewood at
98 400 °C and 300 bar using potassium carbonate as a catalyst and sodium hydroxide for pH adjustment,
99 as previously reported in the literature.²² Details on the effect of the operating parameters on the
100 hydrothermal liquefaction process can be found in the work of Jensen et al.⁶ As a difference compared
101 to the previous work where sCO₂ was used to fractionate the bio-crude obtained in this thermochemical
102 process, in the present work the bio-crude underwent neither dewatering nor demetalization. Therefore,
103 it is a raw bio-crude simply obtained by gravimetric separation from the aqueous phase downstream of
104 the HTL reactor. It appears as a black high-viscosity liquid (Figure 1a), even though less viscous than

105 the bio-crude of the previous work,²² and as a stable emulsion of water in oil, since no phase separation
106 was observed during 6 months of storage.



107

108 **Figure 1.** a) The HTL bio-crude used in this work; b) Example of the residue after sCO₂ extraction,
109 tetrahydrofuran evaporation and mortar grinding. The example refers to the run at 450 bar and 100 °C.

110 2.1.2. Chemicals

111 Carbon dioxide (CO₂, 99.7 %) used for the supercritical extractions was purchased from Air Liquide
112 (Denmark). Diethyl ether (DEE, 99 %) from VWR and pyridine (ACS grade) from Hach were used as
113 solvents for the GC-MS analysis, while vanillin (99.8 %) and myristic acid (99 %) from Sigma Aldrich
114 were used as internal standards. N,O-Bis(trimethylsilyl)trifluoroacetamide (BSTFA, 98.5 %) from
115 Sigma Aldrich was used to derivatize samples. HYDRANAL Titrant 2 and Solvent oil from Fluka, as
116 well as the Aquastar 1 % standard from Merck were used for the Karl Fischer titrations (KF). The
117 elemental analyser was calibrated with the PerkinElmer Cystine 4G powder. Tetrahydrofuran (THF,
118 99.9 %) from VWR was used as solvent for retrieving the residue inside the sCO₂ extractor at the end
119 of each extraction. Ethylene glycol (glycol, 98%) from VWR was used to prepare the aqueous solution
120 (1:1 by mass) employed as cooling fluid in the cold trap described in Section 2.2. Tetrabutyl-
121 ammonium-hydroxide (TBAOH) 0.1 M in 2-propanol/methanol from Merck and tetraethyl ammonium
122 bromide (TEABr) 0.4 M in ethylene glycol (Metrohm) were used as titrant and electrode electrolyte for

123 the total acid number (TAN) measurements. Toluene (99.5 %) and 2-propanol (99.8 %) from VWR
124 were used as solvents for the TAN measurements. NIST traceable Metrohm buffers (i.e. pH 4, 7, 9)
125 were used for calibration of the TAN electrode. Methyl ethyl ketone (MEK, 99 %) and methyl isobutyl
126 ketone (MIBK, 99 %) from VWR, as well as THF, were used as solvents to estimate the density of the
127 bio-crude. A 7 M nitric acid aqueous solution was used for acid digestion and the PlasmaCAL multi-
128 element standard from SCP Science was used for the calibration of the ICP-OES instrument.

129 2.2. Supercritical CO₂ Extraction

130 The experimental setup was described in detail in a previous publication.²² Therefore, only a short
131 description of the setup and the experimental method used in this work, together with notes about
132 modifications, is provided here. The apparatus consists of a high-pressure extraction vessel (i.e. the
133 extractor) with a 178 cm³ basket insert, where approximately 50 g of bio-crude were charged prior to
134 an extraction. The basket insert was packed with 6 mm soda-lime glass beads up to approximately 1/3
135 of its height. The glass beads were chosen as an inert packing material that can disperse the bio-crude
136 feed and improve its contact with the flowing sCO₂. A cylindrical filter (pore size 10 μm) is used at the
137 top of the basket in order to prevent entrainment of particles. An automatically controlled heating
138 jacket maintained the extraction temperature, which in this work was in the range 80 to 150 °C. The
139 temperature indication was within ± 0.5 °C of the set value in all extractions. Liquid CO₂ from a dip-
140 tube cylinder was subcooled by means of a heat exchanger fed with cold water (approx. 5 °C), which
141 was provided by a thermostatic bath (Braun Frigomix U) and erogated by an immersion circulator
142 (Julabo ED). Subsequently the CO₂ was compressed by a high-pressure pneumatic pump and fed to the
143 entry port at the bottom of the extractor. The extraction pressure and the solvent flow rate were
144 regulated manually by the pressure of the air supply of the pump and by a micrometering valve

145 downstream the extractor. The extraction pressures selected for this study were 330 bar and 450 bar. At
146 the tested conditions the extractions were smooth, with pressure gauge readings within ± 3 bar of the
147 set value in all runs. The micrometering valve was heated by hot air. The extract was collected in a 20
148 ml sampling vial inserted in a washing bottle immersed in a cold bath that was kept at approximately -
149 10 °C by means of a refrigerating circulator (Lab Companion RW3-0525P). A subsequent gas-washing
150 bottle immersed in the cold bath was packed with 3 – 4 g of cotton wool and aimed at collecting any
151 further condensate, or retaining fine droplets or particles that might be entrained with the CO₂, in order
152 to protect the downstream gas meter. The cotton wool was weighed after each extraction to account in
153 the mass balance. The weight difference of the cotton before and after an extraction was on average 0.1
154 g, while there was no condensate observed in the corresponding gas washing bottle. The gas meter
155 (Ritter TG3, max flow: 6 L/min; min flow: 0.1 L/min; accuracy: 0.5 %) measured the volume of CO₂
156 flowing through it and was equipped with a thermometer for measuring the gas temperature. The CO₂
157 flow rate in this work was in the range 3 to 4 L/min at gas meter conditions, corresponding to mass
158 flow rates in the range 4 to 6 g/min. After the completion of each extraction, the apparatus was
159 depressurized and let to cool down to about 80 °C, the basket insert dismounted and washed with 100 –
160 150 mL of THF in order to retrieve the residue. Preliminary tests showed that allowing the system to
161 cool down to ambient temperature was unfeasible, since the residue solidified incorporating the glass
162 beads and making its own retrieval problematic even with large amounts of THF. The drawback of the
163 recovery of the residue at 80 °C consisted in THF evaporation, together with losses of water contained
164 in the residue, which increased the uncertainty in the mass balance of water, as discussed in Section 3.
165 For extraction D (see Section 3.2), a small sample (approx. 1 g) of the mixture THF + residue was
166 saved for KF analysis, prior to solvent evaporation. THF was then separated from the residue by rotary
167 vacuum evaporation at 50 °C. The amount of THF in the mixture was estimated by subtracting the

168 mass of the residue after evaporation from the mixture THF + residue before evaporation. After the
169 evaporation of THF, the residue appeared as a dry solid. It was ground in a mortar to obtain a fine
170 powder (Figure 1b) and to ensure representative sampling for analysis.

171 2.3. Analytical characterization

172 2.3.1. Elemental analysis

173 Elemental analysis (EA) was performed with a PerkinElmer 2400 Series II CHNS/O analyser coupled
174 with a PerkinElmer AD-6 Autobalance. Carbon, hydrogen and nitrogen were measured while oxygen
175 was calculated by difference. Sulphur was in all measurements under the detection limit of the
176 instrument and was omitted, since it is not expected to be present in this type of bio-crude. The
177 instrument was calibrated by the Cystine standard (single point calibration) prior to each series of
178 measurements, which were performed at least in triplicate. The Absolute Relative Deviation (ARD)
179 between the measured elemental mass fractions of the standard compared to the theoretical values for
180 C, H, and N was on average 0.4 %. The Relative Standard Deviation (RSD) on oxygen was 17 % for
181 the feed bio-crude, whereas it was on average 21 % for the extracts and 6.4 % for the residues.

182 2.3.2. Water content

183 A Metrohm 870 KF Titrino Plus, coupled with a Metrohm 860 KF Thermoprep, was used for the KF
184 water determination. The instrument was calibrated regularly with the Aquastar 1 % standard, as well
185 as controlled with the standard prior to daily measurements. The ARD between the measured mass
186 fraction of water of the standard and its theoretical value was always below 3 %. Approximately 0.1 g
187 of bio-crude, extracts and residue (after solvent evaporation) were analysed. A sample of
188 approximately 0.1 g was titrated also for the residue + THF mixture sample, in the case of Extraction D

189 (see Section 3.2). In this case, however, also the pure THF used for retrieving the residue was titrated in
190 order to account for water already contained in the solvent. All KF measurements were performed at
191 least in triplicate. The RSD for the feed bio-crude was 4.9 %, whereas it was on average 4.8 % for the
192 extracts and 1.4 % for the residues.

193 2.3.3. Acid number measurements

194 The acid number measurements were carried out by potentiometric titration on a Metrohm Titrand
195 888 equipped with a Metrohm Solvotrode, following a procedure based on a modification of ASTM
196 D664 test method B, which was developed in a previous work.²² The titration solvent was a mixture of
197 toluene, 2-propanol and demineralized water (100:99:0.5, by volume), instead of pure 2-propanol,⁴² as
198 this mixture proved more effective in dissolving the bio-crude and its extracts of this work.
199 Approximately 0.1 g of bio-crude, extract or residue were diluted in 50 ml of the titration solvent and
200 titrated. The method allows for determination of two acid numbers: the carboxylic acid number (CAN)
201 and the total acid number (TAN), both expressed as mg KOH/g. The difference between TAN and
202 CAN is the acid number that corresponds to the phenolic nature of acidity (PhAN), which is an
203 important factor in lignocellulosic bio-crudes. The electrode was calibrated with 3 NIST traceable
204 buffers (i.e. pH 4, 7, 9) and the calibration always demonstrated an R-squared (R^2) of at least 0.999
205 between pH and the measured electrical potential. According to the method, two inflection points are
206 observed during the titration, which correspond to CAN and TAN, respectively. All TAN
207 measurements were performed at least in triplicate. The RSD on TAN, CAN and PhAN for the feed
208 bio-crude was 2.1 %, 1.4 % and 2.9 %, respectively. The average RSD on TAN, CAN and PhAN for
209 the extracts was 1.6 %, 1.0 % and 1.6 %, respectively. The average RSD on TAN, CAN and PhAN for
210 the residues was 1.3 %, 0.8 % and 1.0 %, respectively.

211 2.3.4. Density measurement

212 The density measurements were performed following a procedure developed before.²² The bio-crude
213 density was measured with an Anton Parr DMA 35 Ex densitometer after dilution in three solvents
214 (THF, MIBK and MEK), 1:1 by mass in each. Due to the small quantity of the sCO₂ extracts, their
215 density was calculated by accurately measuring the mass of a volume displaced by a precision pipette
216 (Gilson Microman M1000). The mass was weighed on an analytical balance (OHAUS PA224C) and
217 the capillary piston used for each measurement was calibrated with distilled water in order to calculate
218 accurately the displaced volume. The relative standard deviation (RSD) of triplicate pipetting of
219 distilled water was always lower than 1 %. Density of pure water at the laboratory ambient conditions
220 was taken from NIST.⁴³ All density measurements were performed in triplicate. The RSD for the feed
221 bio-crude was 0.9 %, whereas it was on average 1.4 % for the extracts.

222 2.3.5. Metal content determination by ICP-OES

223 The metal content of the feed and of all the extracts, together with the metal content of the residue of
224 selected extractions, was determined by Inductively Coupled Plasma - Optical Emission Spectrometry
225 (ICP-OES), utilizing a PerkinElmer Optima 8000 system. The content of Potassium (K) and Sodium
226 (Na) was measured, since they were expected due to the use of K₂CO₃ as catalyst and NaOH as pH
227 adjuster in the HTL process. Additional metals subjected to quantitation were Aluminium (Al), Iron
228 (Fe), Magnesium (Mg) and Titanium (Ti), since they are expected to derive from wear of equipment
229 and natural presence in the pinewood biomass.²⁴ Samples were prepared by acid digestion and dilution.
230 Approximately 0.5 g of sample were digested in an autoclave in 20 ml of 7 M aqueous nitric acid for
231 30 minutes at 120 °C and 2 bar. A blank of the nitric acid solution was digested as well for each set of
232 samples and non-zero concentrations were subtracted from the sample measurement in order to account

233 for baseline errors. The digested samples were diluted with distilled water in a volumetric flask (Class
234 A), and filtered by filter paper (pore size 4-12 μm). Dilution to 50 ml was performed for the bio-crude
235 and the residues, while dilution to 25 ml was applied for the extracts. In case of visually observed
236 turbidity of the solution, which was assumed to be due to organic particles, a second filtration was
237 performed to acquire a transparent fluid to protect the plasma torch. In order to ascertain the
238 reproducibility of the sample preparation procedure, eight samples of different mass of the feed bio-
239 crude (i.e. 0.4 to 1 g) were digested and analyzed. The extracts and residues were measured in
240 duplicate. The standards solutions used for calibration were prepared by diluting the PlasmaCAL
241 standard in demineralized water and measured in triplicate. The range was 0.2 to 2 mg/L for all the
242 metals, with the exception of Fe (0.2 to 10 mg/L), K (2 to 100 mg/L) and Na (2 to 10 mg/L). The R^2 for
243 all elements was always above 0.999 except for Na, which was however always above 0.988. The
244 Relative Standard Deviation (RSD) of the triplicate measurements of the calibration standards was
245 always lower than 1 %, while the ARD with respect to the analyzed standard value was always between
246 0 and 4 % for all metals except Na. In fact, Na had a higher ARD (always lower than 20 %) which is
247 assumed to be an inherent instrument inaccuracy for Na measurement. High uncertainty in Na
248 concentration by ICP measurements has been reported in literature for fast pyrolysis oil of woody
249 biomass.⁴⁴

250 2.3.6. Component identification by GC-MS

251 GC-MS analysis was performed for the identification and quantitation of the GC-detectable fraction
252 (i.e. the volatile fraction) of the bio-crude feed and the extracts. In addition, GC-MS after silylation was
253 performed to identify and quantify free fatty acids and a few phenolic components for which the ion
254 peaks had better resolution than in the non-silylated samples. The analysis was performed on a

255 PerkinElmer Clarus 680 GC coupled with a PerkinElmer Clarus SQ 8T MS. For the analysis of the
256 feed, the bio-crude was extracted with DEE (bio-crude to solvent ratio approximately 1:50 by mass)
257 and the resulting DEE-rich mixture was filtered with a syringe filter (pore size 0.45 μm). The amount
258 of the DEE-soluble fraction of the bio-crude was determined gravimetrically from the filtrate, after
259 evaporation of the solvent overnight in a fumehood. All sCO_2 extracts were instead fully soluble at a
260 1:10 extract to DEE ratio (mass basis). GC-MS samples were prepared by mixing approximately 0.1 g
261 of the DEE-soluble fraction of the feed, or approximately 0.1 g of extract, with approximately 0.7 g a
262 of a DEE solution containing a known amount of vanillin (1 wt%) as internal standard (IS). Vanillin
263 was selected as IS as most of the identified components were oxygenated aromatics with some degree
264 of similarity to vanillin, with vanillin being however not present in the bio-crude samples, not
265 overlapping with chromatographic peaks of species contained in the bio-crude samples. With regard to
266 the GC-MS after silylation, the feed and extract samples were silylated as follows: about 0.1 g of each
267 sample were dried in a heating cabinet for 2 h at 120 $^\circ\text{C}$, then diluted in pyridine, which contained a
268 known amount of myristic acid (1 wt%) as IS, and derivatized with BSTFA at 60 $^\circ\text{C}$ for 20 minutes.
269 Myristic acid was selected as IS as the GC-MS analysis after silylation was aimed at fatty acids, with
270 myristic acid being however not present in the bio-crude and not overlapping with chromatographic
271 peaks of species contained in the bio-crude samples. The mixture ratio of sample – pyridine – BSTFA
272 was 1:1:1 in mass basis. The derivatized samples were further diluted in DEE (1:25 by mass). For all
273 samples, 1 μl was injected in a PerkinElmer Elite 5 column (30 m, 0.25 mm ID, 0.1 μm), with the
274 temperature ramping from 40 $^\circ\text{C}$ to 250 $^\circ\text{C}$ at a rate of 10 $^\circ\text{C}/\text{min}$. The initial temperature was held for
275 3 min while the final temperature was held for 6 min. The injector was maintained at 300 $^\circ\text{C}$ and the
276 helium carrier gas at 1.0 ml/min. The mass fraction of the identified analytes i was calculated as: $w_i =$
277 $w_{IS} \cdot A_i / A_{IS}$, where A_i and A_{IS} are the chromatographic areas of the analyte i and the IS, respectively,

278 whereas w_{IS} is the mass fraction of the internal standard (vanillin for pure samples, myristic acid for
279 derivatized samples). Triplicate GC-MS measurements were performed for all samples in random
280 consecution in order to account for random GC response differences.

281 3. Results and discussion

282 3.1. Characterization of the feed bio-crude

283 Table 1 reports the measured bulk properties of the bio-crude feed, including the DEE-soluble fraction,
284 density, TAN, CAN, PhAN, water and metal content. In addition, the elemental carbon (C), hydrogen
285 (H), nitrogen (N) and oxygen (O) mass fractions, as well as the H/C and O/C ratios, are reported on a
286 water-free basis. As can be seen, the density of this bio-crude is approximately 1030 kg/m^3 , which is in
287 line with values reported for HTL bio-crudes from lignocellulosic biomass, reported in the range 970 to
288 1140 kg/m^3 .^{5,17,20} The TAN value of 97 mg KOH/g is within the values reported in literatures, which
289 range from 30 to 150 mg KOH/g for HTL lignocellulosic bio-crudes.^{5,18,45} With regard to the elemental
290 composition, the mass fractions are also in line with typical woody HTL bio-crudes (i.e. C: 0.76 – 0.84;
291 H: 0.07 – 0.10; N: 0.002 – 0.030; O: 0.05 – 0.15).^{5,7,17,18}

292 **Table 1.** Bulk properties at ambient conditions, elemental composition on a water-free basis and metal
293 mass fraction of the feed bio-crude with standard deviations.

Property		Metal content (mg/kg)	
DEE soluble fraction	0.70 ± 0.03	Al	40 ± 9
Density (kg/m^3)	1030 ± 9	Fe	190 ± 20
TAN (mg KOH/g)	97 ± 2	K	3400 ± 400

CAN (mg KOH/g)	42 ± 1	Mg	96 ± 20
PhAN (mg KOH/g)	56 ± 2	Na	3800 ± 500
Water content (wt%)	5.7 ± 0.4	Ti	40 ± 3
C mass fraction	0.80 ± 0.01	Total metals	8500 ± 800
H mass fraction	0.08 ± 0.01		
O mass fraction	0.10 ± 0.02		
N mass fraction	0.017 ± 0.005		
H/C	1.2 ± 0.1		
O/C	0.09 ± 0.02		

294

295 As can be seen in Table 1, the bio-crude exhibits a water content of almost 6 wt%, which is at the lower
 296 range of typical reported values for HTL lignocellulosic bio-crudes (i.e. 5 – 15 wt%).^{4,5,7,17} In addition,
 297 the bio-crude exhibits a high metal content of around 0.85 wt%, with potassium (K) and sodium (Na)
 298 constituting more than 90 % of the total. The metal content is dependent on the biomass ash content,
 299 but since woody biomass has typically low ash,⁴⁶ the high metal content mostly originates from the
 300 chemicals used in the HTL process. This behaviour was observed by Déniel et al.²¹, who performed
 301 HTL of blackcurrant pomace and observed ash contents in the bio-crude increasing (i.e. from 0.1 to 5.3
 302 wt%) with sodium hydroxide added (i.e. from 0 to 9 wt%). With regard to Mg, it is known to bind with
 303 organic molecules in biomass,⁴⁷ while Al and Fe are typically introduced during the harvest and
 304 processing of the biomass.²⁴ Ti is one of the less abundant metals in biomass,⁴⁷ which is assumed to be
 305 introduced by equipment wear. The presence of Mg, Al, Fe, Ti, although in relatively small amount
 306 (0.03 wt% in total), is confirmed in this work.

307 In total, 46 components were identified by GC-MS in the DEE-soluble fraction of the feed. Detailed list
308 of the components along with retention time (RT), classification, molecular weight (MW), chemical
309 formula, CAS registry number and their mass fraction (wt%) in the feed bio-crude is reported in the
310 supporting information (Table S1). The identified components constitute 19.3 wt% of the feed bio-
311 crude. The unidentified components of this volatile fraction correspond to a chromatographic area that
312 is about twice as large as the identified fraction, which means that, as a rough estimation, about 60 wt%
313 of the bio-crude can be assumed as volatile. The identified components were lumped into 10 categories
314 according to their chemical functionalities: 1) Cyclic aliphatic (C6 – C9) ketones, saturated or
315 monounsaturated (Ketones, K); 2) Alkylbenzenes (AB); 3) Phenol and alkylphenols (Phenols, P); 4)
316 Guaiacol and alkylguaiacols (Guaiacols, G); 5) Benzenediols and acetyl derivatives of benzenediols
317 (BD); 6) 2- and 3-ring aromatic hydrocarbons (PAH); 7) Dehydroabeityl alcohol (ArAl); 8) Short chain
318 fatty acids, in the range C2 – C8 (SFA); 9) Long chain fatty acids, in the range C16 – C18 (LFA); 10)
319 Dehydroabiatic acid (ArAcid).

320 The largest fraction of the identified components is constituted by PAHs, which account for 9 wt% of
321 the bio-crude. Even though such components are not often reported often, some have been reported by
322 Pedersen et al.¹⁸ in the distillation residue of woody HTL bio-crude. Retene has been reported in the
323 HTL bio-crude of softwood lignin.⁴⁸ Retene and phenanthrenes are possibly the degradation products
324 of dehydroabiatic acid in the biomass, since they are typically found as products of its thermal
325 degradation (e.g. wood smoke).^{49,50}

326 Single-ring aromatic hydrocarbons (alkylbenzenes, AB) are also found, albeit in lower amount (1
327 wt%). Aliphatic hydrocarbons are not observed. Fatty acids (SFA + LFA) are the second most
328 abundant group, accounting for almost 4 wt% of the oil, with the LFA being largely predominant (3.75

329 wt%). Fatty acids are typically one of the most abundant classes in bio-crudes,⁵¹ although their mass
330 fractions are not often reported. Dehydroabiatic acid and dehydroabeytil alcohol are also observed in
331 remarkable amount, 1.8 wt% and 0.4 wt%, respectively. Abietane skeleton diterpenoids are major
332 structures of conifers such as pine,⁵⁰ and dehydroabiatic acid is therefore expected to be present in the
333 pine biomass of the bio-crude used in this work. The presence of dehydroabiatic acid in the bio-crude
334 suggests that it remains unconverted, to some extent, during the HTL process. Ketones are always
335 present in lignocellulosic bio-crudes. However, even though they are numerous, they are in low
336 amount, summing up to 0.5 wt% of this oil. Single-ring phenolics (alkylphenols, catechols and other
337 types of benzenediols, and guaiacol) account altogether for 2.6 % of the bio-crude. Alkylphenols,
338 catechols and guaiacols are typically observed in HTL of softwood lignin,^{3,14,48} with the ratio catechols
339 to guaiacols increasing with the HTL reaction temperature.^{14,48} Their presence and the low
340 guaiacols/catechols ratio is therefore qualitatively in line with the high-temperature hydrothermal
341 decomposition of the lignin contained in the original biomass of this work.

342 3.2. Extraction conditions and yields

343 The experimental conditions and mass balances for each supercritical extraction are reported in Table
344 2. Four different extraction temperatures (i.e. 80, 100, 120 and 150 °C) were tested at two pressures
345 (i.e. 330 and 450 bar). The lower pressure (330 bar) was chosen to be within the typical pressure range
346 of the HTL process,¹⁹ therefore allowing the investigation of the sCO₂ extraction at pressure levels
347 comparable to the HTL reactor, as higher pressures in the downstream separation would be less
348 favourable for process economics. The higher pressure (450 bar) was selected on the basis of previous
349 works,^{22,37} which showed promising results in terms of attainment of high extraction yields. The
350 duration of the extractions was between 5.3 and 6.4 hours. Table 2 also reports: the density of pure CO₂

351 at the operating conditions of the extraction (ρ); the average solvent mass flow rate (Q); the mass of
 352 feed bio-crude charged in the extractor at the beginning of an experiment (F); the mass of the four
 353 extracts collected in each extraction (E1, E2, E3 and E4), with the exception of run A where only three
 354 extracts were collected. Run A was the extraction with the lowest yield and the third sampling vial (i.e.
 355 E3) was maintained for a longer period to avoid ending up with E4 sample mass inadequate for
 356 analysis. The mass balance discrepancy (losses, L) of each run is also reported, together with the total
 357 solvent-to-feed ratio (i.e. at the end of the run) and the total extraction yield. The total extraction yield
 358 is defined as the ratio of the total mass of the collected extracts to the mass of the feed. It is therefore
 359 determined gravimetrically. Data from Table 2 were also used to calculate the Vapour Phase Loading
 360 (VPL) as the extractions progress. VPL is defined as the ratio of the mass of extract in a given time
 361 interval over the mass of solvent flowed in the same interval. VPL values were also used to evaluate
 362 the reproducibility of the extraction procedure. In this regard, six repetitions of Run H were carried out
 363 and the RSD on VPLs were found to be: 7.1 % for extract 1 (E1); 11.6 % for extract 2 (E2); 14.0 % for
 364 extract 3 (E3); 11.3 % for extract 4 (E4).

365
 366 **Table 2:** Experimental extraction conditions and results. Temperature (T); pressure (P); CO₂ density
 367 (ρ); average CO₂ mass flow rate (Q); mass of feed (F); mass of extract samples (E1, E2, E3, E4); mass
 368 of residue (R); losses (L); solvent-to-feed ratio (S/F); total yield (Y_T).

Run ID	A	B	C	D	E	F	G	H
T (°C)	80	100	120	150	80	100	120	150
P (bar)	330	330	330	330	450	450	450	450

ρ (kg/m³)^a	773	696	623	531	851	790	731	650
Q (g/min)	5.2	5.5	5.0	4.7	5.7	5.9	5.0	4.8
F (g)	48.9	52.6	51.3	53.6	53.9	51.5	54.2	51.9
E1 (g)	6.6	5.7	7.7	5.4	5.3	8.4	6.9	6.6
E2 (g)	6.1	5.9	5.3	6.9	5.3	5.8	6.4	7.6
E3 (g)	8.9	6.0	5.6	5.0	5.3	5.5	6.9	6.2
E4 (g)	-	6.2	5.0	7.5	8.1	7.2	7.8	7.3
R (g)	23.1	24.4	22.8	23.8	23.9	21.0	22.2	18.0
L (%)	8.2	6.5	9.4	9.0	9.4	7.0	8.5	12.0
S/F (g/g)	30.2	36.5	36.3	31.6	32.4	36.7	33.3	30.0
Y_T (%)	44.1	45.1	46.0	46.3	47.3	52.4	51.5	53.4

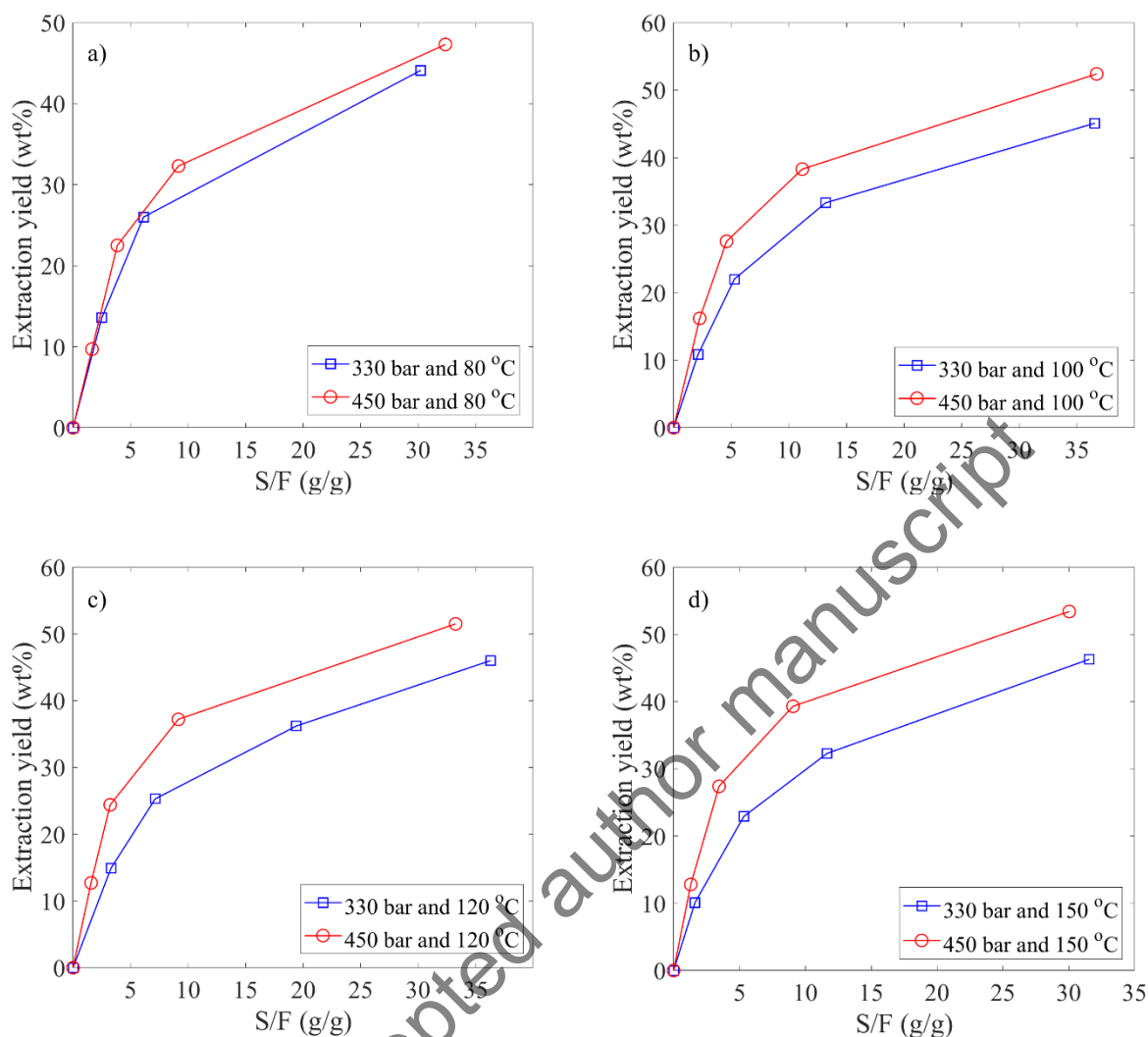
^a Taken from NIST ⁴³;

369 In Table 2, it can be seen that the highest extraction yield of 53.4 % is not achieved at the highest
370 solvent density, but in fact at the highest temperature and in combination with high pressure. This
371 observation highlights the importance of high temperatures for sCO₂ separation of bio-crudes and it is
372 in line with previous works,^{22,37} where extraction yields up to 48.9 % have been achieved at 448 bar
373 and 120 °C while low efficiency and bad operability were observed below 80 °C. Importantly, not only
374 was Run H characterized by the highest yield but also by the lowest S/F (i.e. 30 g/g). These results
375 indicate that operating conditions of the downstream sCO₂ separation at pressures higher than the
376 pressure of the HTL reactor should not be discarded a priori in the design of the process.

377 In Figure 2, the extraction yield is plotted vs. the solvent to feed ratio at the four different temperatures
378 and the two pressures. In all cases, the effect of pressure is beneficial for the extraction efficiency,

379 showing higher extraction yields at given S/F values. This is a general feature in sCO₂ separation
380 processes, since higher pressures at given temperatures lead to higher solvent density and increased
381 solvent power. The perusal of Figure 2 also shows that the increase in process efficiency with pressure
382 at given temperature is more pronounced at higher temperatures. This is due to the isothermal variation
383 of the solvent density, which is monotonically increasing with temperature, ranging from 78 to 119
384 kg/m³ as temperature increases from 80 to 150 °C. The increase of the yield for given S/F as pressure
385 increases at constant temperature, which is to say the increased extract to solvent ratio (E/S) with
386 pressure, is typically observed in sCO₂ extraction processes. The primary reason is the increase in
387 solubility of extractable species in the supercritical solvent. However, it is recognised that the
388 extraction yield is affected by both the solubility of extractable species and by mass transfer parameters
389 .⁵²

Accepted author manuscript



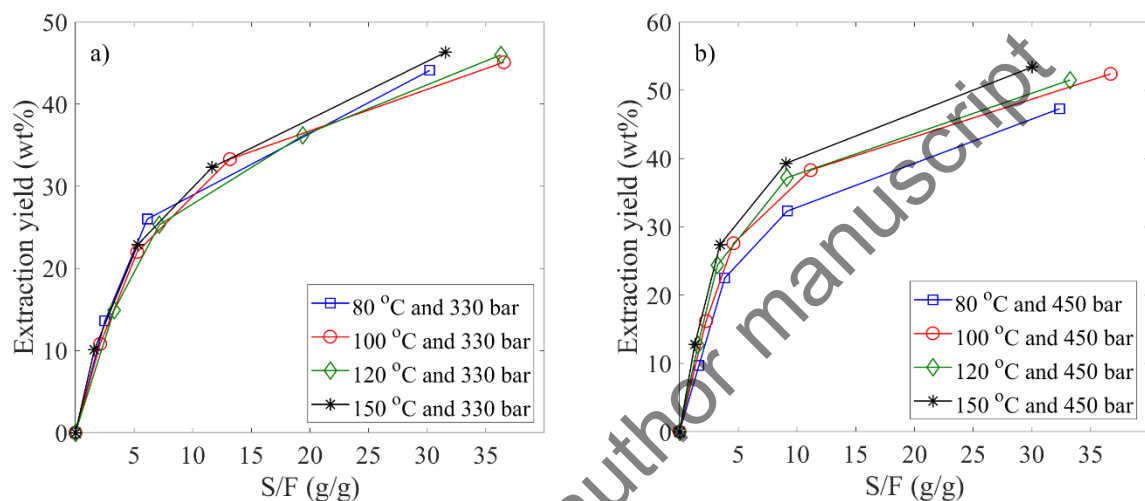
390

391

392 **Figure 2.** Pressure effect on the extraction yield vs. solvent to feed ratio (S/F) at: a) 80 °C; b) 100 °C;
 393 c) 120 °C and d) 150 °C.

394 In order to visualize this combined effect, Figure 3 shows the extraction yield against S/F at the two
 395 studied pressures (i.e. 330 and 450 bar). At 330 bar it is observed that, even though the increase of
 396 temperature decreases the solvent density, the extraction yields are comparable for all temperatures.
 397 This could indicate that the solubility of the bio-crude at this pressure reduces with temperature, but the
 398 mass transfer parameters improve enough to counteract the reducing solubility. Contrary to the

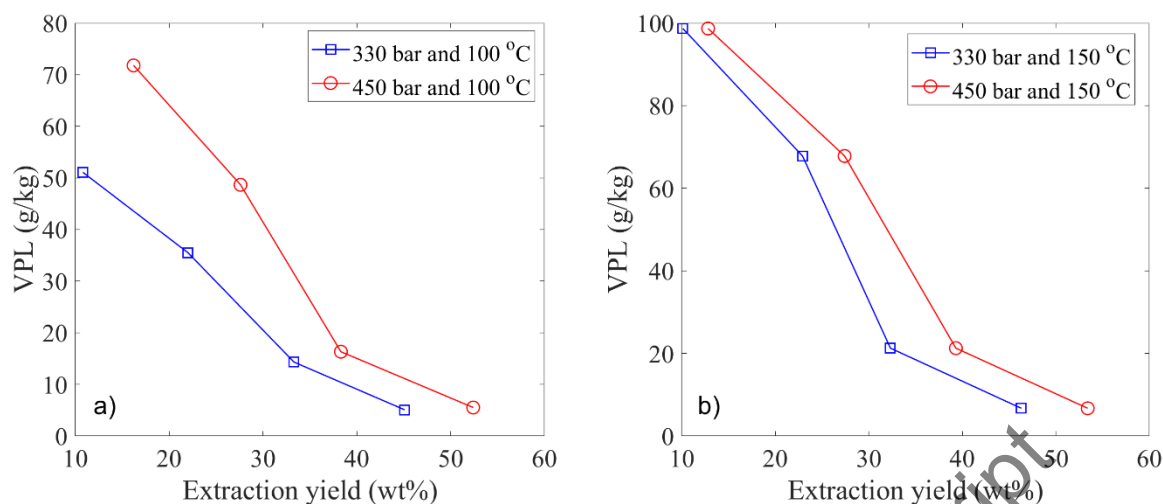
399 behaviour at 330 bar, at 450 bar the extraction yield slightly increases with temperature. This could be
400 either due to a crossover pressure between 330 and 450 bar that results to solubility increasing with
401 temperature, or due to mass transfer improvements prevailing to the solubility decrease with
402 temperature. Phase equilibrium measurements of the solubility of this type of bio-crude in sCO₂ are not
403 available in the literature and they would be needed to prove the above-mentioned hypotheses.



404

405 **Figure 3.** Temperature effect on the extraction yield vs. solvent to feed ratio (S/F) at: a) 330 bar and b)
406 450 bar.

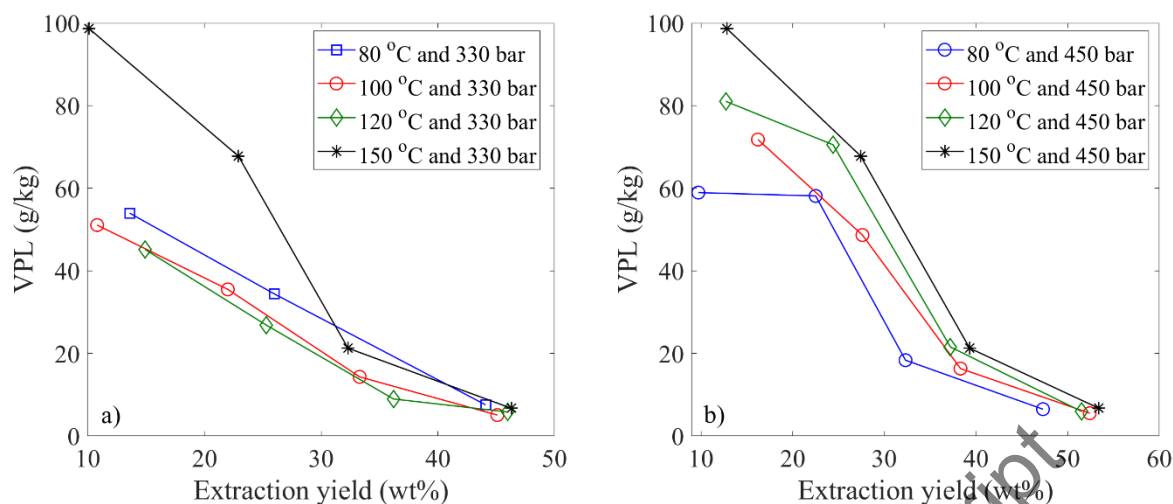
407 In theory, the slope of the curves in Figure 2 and Figure 3 (dE/dS) indicates the Vapour Phase Loading
408 (VPL), i.e. the instantaneous value of the mass of components extracted per unit mass of solvent. The
409 collection of a number of extracts per each run allowed to estimate average VPL values ($\Delta E/\Delta S$) as the
410 extraction proceeds. Results are presented for the extractions at 100 °C (Figure 4a) and 150 °C (Figure
411 4b) and at 330 (Figure 5a) and 450 bar (Figure 5b). Similar trends as Figure 4 are observed at all
412 temperatures studied.



413

414 **Figure 4.** Pressure effect on the vapour phase loading (VPL) vs. extraction yield at: a) 100 °C; b) 150
 415 °C.

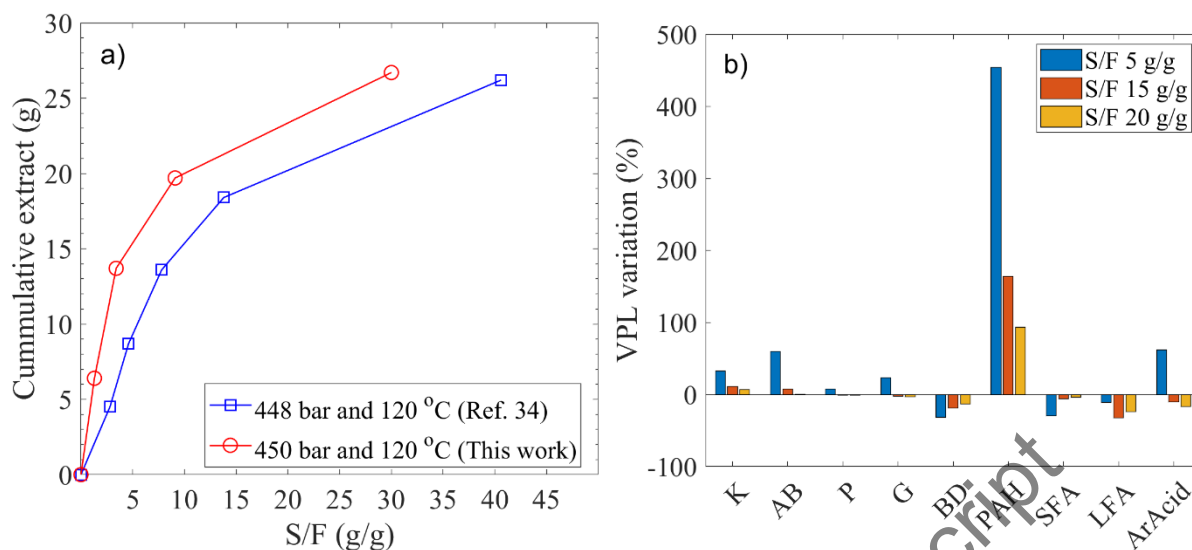
416 As usual, VPL values decrease during the extraction, as the unextracted bio-crude remaining inside the
 417 extractor becomes progressively heavier. As can be seen from Figure 4, higher pressure at given
 418 temperature leads to higher VPL values, which resulted to the highest extraction yield with the least
 419 solvent used in Run H. On the other hand, the effect of temperature is more complex as can be seen in
 420 Figure 5. Figure 5b shows that higher temperatures affect positively the VPL at 450 bar, especially in
 421 the early stages of the extraction. Whereas at 330 bar (Figure 5a) this effect is only observed at the
 422 highest temperature (i.e. 150 °C) and for extraction yields below approximately 30 wt%.



423

424 **Figure 5.** Temperature effect on the vapour phase loading (VPL) vs. extraction yield at: a) 330 bar and
 425 b) 450 bar.

426 An interesting observation arises when the results of this work at 120 °C and 450 bar are compared
 427 with an extraction run carried out at basically same conditions (120 °C and 448 bar) on a dewatered
 428 bio-crude (water content 2.7 %), presented in a previous work.³⁷ In Figure 6a, the cumulative extract is
 429 plotted against S/F for a normalized feed mass (i.e. 50 g). It can be seen that the extraction is more
 430 efficient for the non-dewatered bio-crude of this work. The results of this work show an increase of
 431 extract in the range 3 to 6 g, for given S/F values ranging from 1.3 to 30. The difference in water
 432 content for 50 g of the two bio-crudes is 1.5 g. Considering that the variation of the extract mass is 2 to
 433 4 times higher than the water content in the feed, it is apparent that the increase in the extract cannot be
 434 entirely attributed to the extraction of water itself. Therefore, the presence of water actually enhances
 435 the extraction of other molecules contained in the bio-crude feed.



436

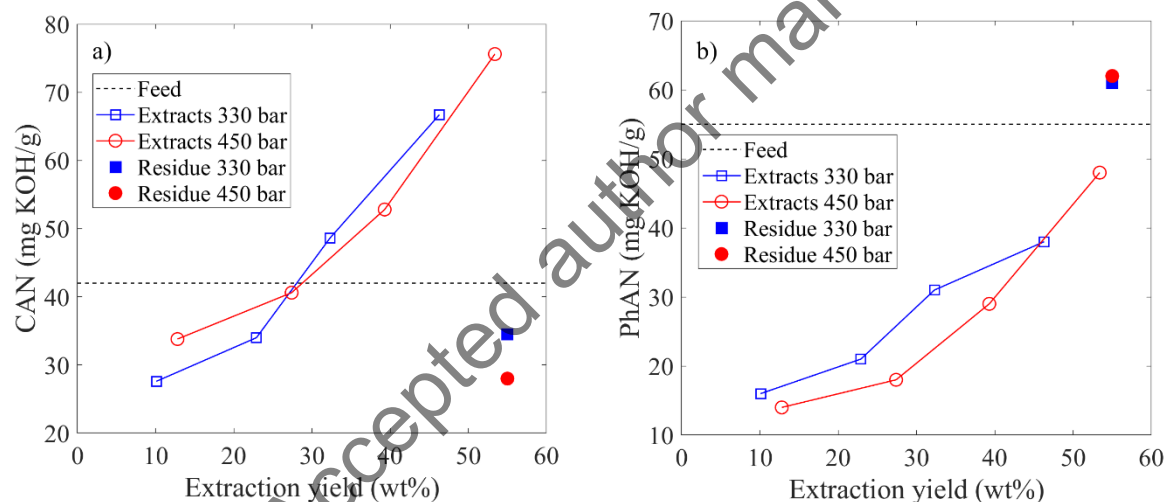
437 **Figure 6. a)** Cumulative extract mass (normalized to 50 g feed) vs. S/F for extraction of dewatered bio-
 438 crude (2.7 wt% water)³⁷ and the bio-crude of this work (5.7 wt% water); b) Vapour phase loading
 439 (VPL) variation of chemical classes between dewatered bio-crude³⁷ and the bio-crude studied in this
 440 work. Ketones (K); Alkylbenzenes (AB); Phenols (P); Guaiacols (G); Benzenediols (BD); 2- and 3-ring
 441 aromatic hydrocarbons (PAH); Short chain fatty acids, in the range C2 – C8 (SFA); Long chain fatty
 442 acids, in the range C16 – C18 (LFA); Dehydroabiatic acid (ArAcid).

443 This enhancement can be discussed in further detail with the aid of Figure 6b, where the variation of
 444 VPL, in the two above-mentioned experiments, is shown for specific chemical classes at different S/F
 445 ratios. In Figure 6b, nine out of the ten classes defined in this work are represented, since no aromatic
 446 alcohols were reported in the previous work. The major observation from Figure 6b is that the higher
 447 water content enhances dramatically the VPL of the non-polar hydrocarbons (i.e. AB and PAH). In
 448 addition, components of low polarity (e.g. K, P, G) are extracted more efficiently. The more polar
 449 components (i.e. BD, SFA and LFA) have in general higher VPL for the bio-crude with the lower
 450 initial water content. In all cases the benefit of the presence of water is reduced while the extraction

451 progresses, which is in line with the slope in the curves of Figure 6a, and suggests that this effect
452 becomes less pronounced as the unextracted residue becomes drier. The above indicates that the
453 application of sCO₂ extraction on the non-dewatered bio-crude leads to both increased VPL and
454 selectivity with respect to polar and apolar components.

455 3.3. Bulk properties and elemental composition

456 The values of CAN and PhAN for the extracts increase with the extraction yields (E/F) at all
457 conditions. As an example, the CAN and PhAN values of the extractions at 150 °C are plotted vs. the
458 extraction yield and shown in Figure 7.



459

460 **Figure 7.** Effect of pressure on a) CAN vs. extraction yield and b) PhAN vs extraction yield at 150 °C

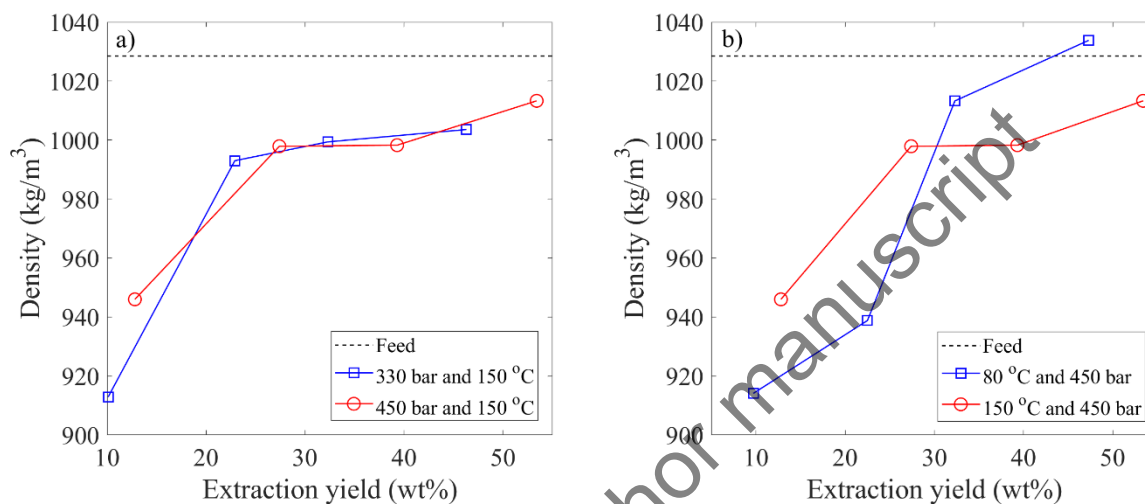
461 CAN values of the first extracts range from 28 to 41 mg KOH/g, which are values always lower than
462 the CAN value of the feed (42 mg KOH/g). This observation indicates that fatty acids are not
463 preferentially extracted at the beginning of the batch separation process. As the extraction proceeds, the
464 CAN value of the extracts increases, with values ranging from 34 to 41 mg KOH/g for E2, 49 to 53 mg
465 KOH/g for E3 and 67 to 76 for E4 mg KOH/g. The trend of the CAN indicates that fatty acids are

466 progressively more extracted as the extraction proceeds. CAN of the residues ranges from 28 to 35 mg
467 KOH/g, which means that, in most of the cases, the residue is partially depleted of carboxylic acids.
468 When CAN values in this work are compared to those of previous work on a dewatered bio-crude,²² it
469 is observed that in the early stages of the extraction (S/F up to 5 g/g), the literature CAN values are
470 higher (i.e. 37 – 47 mg KOH/g) than those of this work (at similar conditions 80 -120 °C and 255 – 400
471 bar). This further indicates that, at the beginning of the separation process, the fatty acids are less
472 extracted in the presence of higher water content.

473 On the other hand, PhAN values of the extracts are always lower than the value of the feed (55 mg
474 KOH/g). In this case, the values ranges from 14 to 16 mg KOH/g for E1, 18 to 21 mg KOH/g for E2,
475 29 to 31 mg KOH/g for E3 and 38 to 48 mg KOH/g for E4. Consistently, the PhAN value of the
476 residue is higher than the feed, resulting to be in the range 61 to 62 mg KOH/g. Overall, the reduced
477 CAN and increased PhAN in the residue indicates that its type of acidity is shifted towards phenolic
478 nature. The highest value of CAN was observed for extract E4 at 450 bar and 150 °C (i.e. 76 mg
479 KOH/g), while the lowest PhAN was observed for extract E1 for the same extraction (i.e. 14 mg
480 KOH/g). A high CAN and low PhAN is advantageous for hydrotreating since HDO of fatty acids is
481 easier than opening aromatic rings.^{53,54} In addition, the increased PhAN indicates that high molecular
482 weight phenolic components remain in the residue. This fraction is expected to be resistant to HDO, as
483 it was similarly shown for the residue of n-pentane extraction of lignocellulosic bio-crude.⁵⁵

484 The density of the extracts was found in the range of 914 to 1034 kg/m³, increasing with the extraction
485 progression. Most of the sCO₂ extracts exhibit a moderate reduction compared to the feed, with the
486 maximum being a 10 % reduction for early extracts (i.e. E1, E2). The later extracts show a density
487 comparable to the feed, with only the final extracts (i.e. E4) at 80 °C and 300 bar and 100 °C and 450

488 bar exhibiting a density slightly higher than the feed (see example in Figure 8b). The extraction
489 conditions show negligible influence on the density of the extracts. As in the case of acidity, also in the
490 case of density the trends were similar at all experimental conditions. Figure 8a shows an example
491 referred to the extractions at 150 °C, whereas Figure 8b shows two cases at 450 bar.



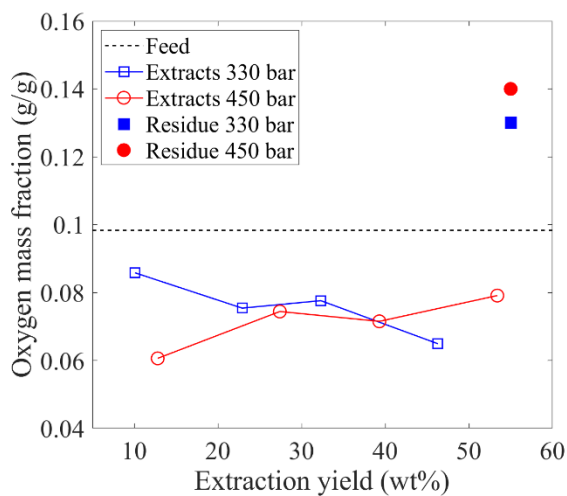
492

493 **Figure 8.** Density vs. extraction yield at: a) Constant temperature (150 °C); b) Constant pressure (450
494 bar).

495 The water content of the extracts was measured for the experimental runs B, E, D, and H and resulted
496 to be in the range 1.3 to 1.8 wt%, with no clear trend with the extraction pressure and temperature.
497 Importantly, the values are consistently and remarkably lower than the water content of the feed (i.e.
498 5.7 wt%). The water content of the residues of the same extractions was measured after evaporation of
499 the solvent used for their recovery. The obtained values were in the range 0.9 to 1.6 wt%. The fact that
500 the water content was observed to decrease both in the residue and in the extract clearly indicates that it
501 was not possible to recover all the water from the system, due to lack of complete recovery in the cold
502 trap and/or water losses during the recovery of the residue at the end of the extraction. The mass

503 balances indicate that approximately 50 % of the water originally in the feed was not retrieved in the
504 extracts and in the residue. For extraction D, the water content of the residue was measured by means
505 of direct KF titration of a sample of THF solution, i.e. before the solvent evaporation. The value was
506 1.2 wt%, while the corresponding value after solvent evaporation was 0.9 wt%. This means that about
507 2% of the water in the feed was lost during the vacuum evaporation, which is not significant with
508 regard to the total water losses. Interestingly, the earlier extracts (i.e. E1, E2) exhibited spontaneous
509 separation of water, with water droplets collecting at the bottom of the storage vials. This was not
510 observed for the later extracts (i.e. E3, E4). This freely separated water was determined for extractions
511 at 150 °C and it was 0.4 g and 0.6 g for extractions H and D, respectively, which corresponds to 13 %
512 and 20 % of the original water in the feed. Even though it was not possible to close the mass balances
513 on water, the results clearly indicate that sCO₂ process co-extracts water from the HTL bio-crude,
514 induce the separation of water from the extracts and allows reducing the water content in the residue as
515 well.

516 The carbon mass fraction in the extracts was in the range 0.80 to 0.81, which are values close to the
517 values of the feed (i.e. 0.80) and the residue (0.78 – 0.79). The hydrogen content (on a water-free basis)
518 is slightly increased in the extracts (0.09 – 0.11), with respect to the feed (i.e. 0.08) and the residues
519 (range 0.07 – 0.08). The oxygen mass fraction of the extracts (on a water-free basis) was for all
520 extractions lower than that of the feed, ranging from 0.05 to 0.07 (vs. 0.10 in the feed). In line with this,
521 the mass fraction of oxygen of the residues increased, ranging from 0.13 and 0.15. The oxygen mass
522 fraction of the extractions performed at 150 °C is plotted in Figure 9 as a function of the extraction
523 yield. Similar trends are observed in all extractions.



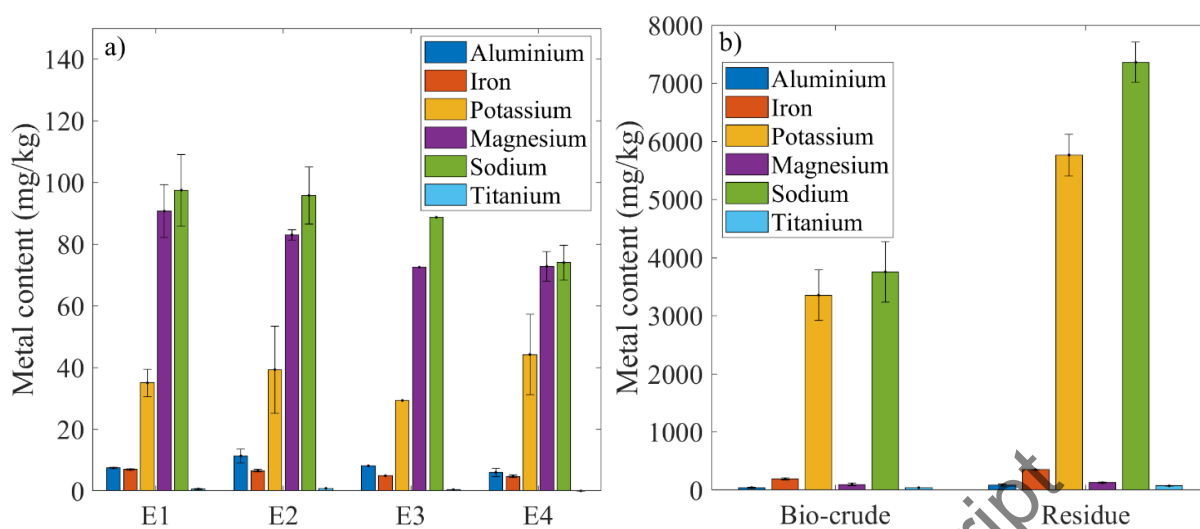
524

525 **Figure 9.** Oxygen content on a water-free basis vs extraction yield for extractions at 150 °C.

526 3.4. Metal content of bio-crude extracts and residues

527 The metal content of extracts and residues was measured for extraction B, D, G and H. In all cases, the
 528 extracts were found almost completely devoid of metals. The metal content was reduced from 95 % to
 529 99 %, compared to the feed value. The analysis of the residues confirmed that the metals are
 530 concentrated in the unextracted phase. The trends were very similar in all runs. As an example, the
 531 results obtained with the extraction at 330 bar and 150 °C are reported in Figure 10.

532 As can be seen in Figure 10, potassium and sodium, which constitute more than 90 % of the metal
 533 content of the feed, are reduced from 3400 mg/kg and 3800 mg/kg down to values ranging from 30 to
 534 40 mg/kg and 70 to 100 mg/kg, respectively. Aluminium, iron and titanium are reduced in the extracts
 535 down to values below 10 mg/kg in all extracts. Interestingly, magnesium remains unchanged, which
 536 suggests that it may be in organometallic components²⁴ that can be solubilized by sCO₂. In all cases,
 537 the total metal content was found to be drastically reduced from 8500 mg/kg down to an average value
 538 of 170 mg/kg.



539

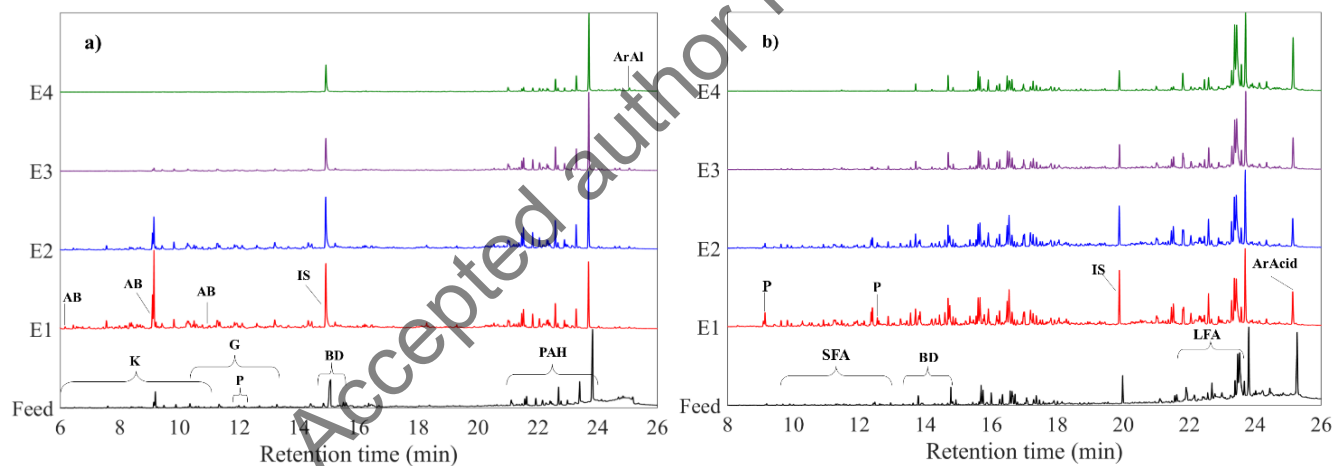
540 **Figure 10:** Metal distribution between bio-crude, extracts (i.e. E1, ..., E4) and residue for the extraction
 541 at 330 bar and 150 °C. Error bars represent the standard deviation of at least duplicate measurements.

542 The small amount of metals in the extracts indicates that either they can be entrained together with fine
 543 water droplets where they are dissolved in, or they are present, albeit in very small amount, as
 544 organometallic components that are soluble in sCO_2 . The 10 μm filter at the top of the basket insert is
 545 expected to act as a factor limiting the entrainment of water droplets.

546 3.5. Chemical composition by GC-MS

547 Figure 11a shows the total ion chromatograms (normalized with respect to the highest peaks) of the
 548 non-derivatized samples of the feed bio-crude and the extracts obtained at 330 bar and 150 °C. Figure
 549 11b shows the corresponding chromatograms for the derivatized (silylated) samples. The trends shown
 550 in Figure 11 are qualitatively representative of all extractions carried out in this work. It is noted that
 551 some classes of components exhibit overlapping Retention Time (RT) ranges, which does not allow
 552 assuming that all components in a certain RT range are expected to belong to a specific class. As can be
 553 seen in Figure 11a, the concentration of lower retention time components (up to 17 min) is increased in

554 the first extract, while it decreases in subsequent extracts. This indicates that these components are
 555 preferentially extracted at the beginning of the process and depleted in the unextracted oil. The peak
 556 areas of higher retention time components (21 – 25 min) increase over time, which is particularly
 557 visible by the increasing difference between the largest peak of the chromatograms (retene at 23.8 min)
 558 and the IS (vanillin at 15.1 min). This indicates that they are not preferentially extracted in the early
 559 stages of the extraction, but are substantially extracted as their concentration in the residue increases.
 560 Similar trend is observed in the derivatized sample (Figure 11b), with light components (RT up to 15
 561 min) extracted preferentially in the early stages while gradually depleted. In this case, the heavy acids
 562 (i.e. LFA and ArAcid, RT above 21 min) are progressively extracted in relatively higher amounts as the
 563 extraction proceeds.



564

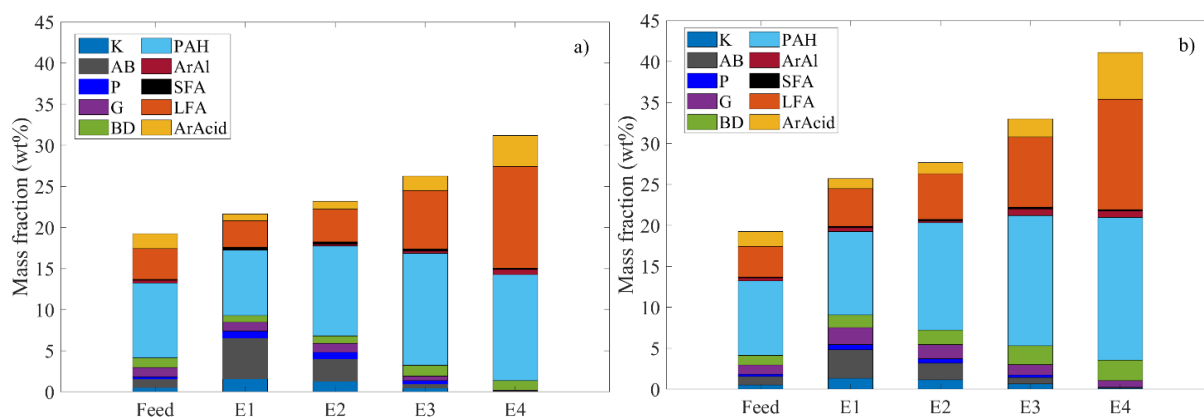
565 **Figure 11.** Chromatograms of feed bio-crude and extracts E1 – E4 of the extraction at 330 bar and 150
 566 °C. a) non-derivatized samples; b) derivatized (silylated) samples. Ketones (K); Alkylbenzenes (AB);
 567 Phenols (P); Guaiacols (G); Benzenediols (BD); 2- and 3-ring aromatic hydrocarbons (PAH); Aromatic
 568 alcohol (ArAl); Short chain fatty acids, in the range C2 – C8 (SFA); Long chain fatty acids, in the
 569 range C16 – C18 (LFA); Dehydroabiatic acid (ArAcid).

570 Figure 12 shows the progress of the mass fractions of the identified classes of components with the
571 extraction time with reference to the extractions at 150 °C, which are taken as a representative example
572 of all extractions. The total identified components in the sCO₂ extracts are in the range 27 wt% to 40
573 wt%, which are higher values compared to the feed (19 wt%). This observation, together with the
574 reduction in density (see Section 3.3) indicate that the extract has lower average molecular weight than
575 the feed. A lower average molecular weight is expected to reduce coking during catalytic
576 hydrotreatment, thus prolonging the lifecycle of the catalyst.²⁵

577 Ketones, alkylbenzenes, phenols, guaiacols and short chain fatty acids are decreasing monotonically
578 with extraction progression, while benzenediols, polyaromatic hydrocarbons, long chain fatty acids and
579 the aromatic acid increase. The aromatic alcohol does not show any specific trend mostly being
580 unchanged between the extracts. In further detail, the mass fractions of the above-mentioned species in
581 the extracts were found in the ranges of: ketones (0.06 – 1.9 wt%); alkylbenzenes (0.05 – 6.6 wt%);
582 phenols (0.03 – 0.9 wt%); guaiacols (0.04 – 2.5 wt%); benzenediols (0.8 – 3.6 wt%); polyaromatic
583 hydrocarbons (8 – 23 wt%); dehydroabetyl alcohol (0.1 – 1.4 wt%); short chain fatty acids (0.09 – 0.3
584 wt%); long chain fatty acids (3 – 14 wt%); dehydroabiestic acid (0.8 – 6 wt%).

585

586



587

588 **Figure 12.** Mass fractions on a water-free basis of the feed and sCO₂ extracts for the experimental runs
 589 at: a) 330 bar and 150 °C; b) 450 bar and 150 °C. Ketones (K); Alkylbenzenes (AB); Phenols (P);
 590 Guaiacols (G); Benzenediols (BD); 2- and 3-ring aromatic hydrocarbons (PAH); Aromatic alcohol
 591 (ArAl); Short chain fatty acids, in the range C2 – C8 (SFA); Long chain fatty acids, in the range C16 –
 592 C18 (LFA); Dehydroabietic acid (ArAcid).

593 Overall, the GC-MS analysis shows that the trend of the separation is mainly determined by molecular
 594 weight, with the lighter components preferentially extracted in the early stages of the extraction. The
 595 polarity plays however an important role as well, as can be observed by the different behaviour
 596 between guaiacols, preferentially extracted in the early stages, and benzenediols, which are more polar
 597 and are extracted at later stages even though having a slightly lower molecular weight.

598 4. Conclusion

599 This work proves that sCO₂ extraction is an effective process for the separation of raw (i.e. non-
 600 dewatered and non-demetalized) HTL lignocellulosic bio-crude. The process is capable of extracting a
 601 large fraction of the bio-crude (yields of extract up to 53 wt%) with relatively low solvent-to-feed ratios
 602 (i.e. 30 to 37 g/g) compared to typical values for sCO₂ extractions. The extracts showed favorable

603 properties towards downstream catalytic hydrotreatment. More specifically, they were drastically
604 demetalized (from 8500 mg/kg down to 170 mg/kg on average), substantially dewatered (from 6 wt%
605 down to 1.3 wt% – 1.8 wt%), exhibited lower oxygen content (from 30 to 50 % reduction on a water-
606 free basis), lower average molecular weight and their acidity was shifted towards carboxylic nature,
607 with a reduction of the phenolic acidity. Interestingly, not only is the sCO₂ process capable of
608 simultaneous demetalization, dewatering and upgrading of the bio-crude, but also the process
609 efficiency was improved, compared to sCO₂ extractions at similar conditions on a dewatered bio-crude.
610 Overall, these properties are expected to lead to longer catalyst life, lower hydrogen requirements and
611 less coking. Experimental studies on hydrotreatment of sCO₂ extracts are needed to confirm the
612 expectations and to provide data allowing to evaluate if the advantages that can be obtained in the
613 hydrotreatment step prevail on the reduced yield of hydrotreatment feed with respect to the initial
614 biomass.

615 Supporting information: List of GC-MS identified components (Table S1)

616 Acknowledgments

617 The authors would like to acknowledge the valuable contribution of Linda Birkebæk Madsen, for
618 performing the elemental analysis for this work.

619

620 References

- 621 (1) Castello, D.; Pedersen, T.; Rosendahl, L. Continuous Hydrothermal Liquefaction of Biomass: A Critical
622 Review. *Energies* **2018**, *11*, 3165. <https://doi.org/10.3390/en11113165>.
- 623 (2) Kim, J. Y.; Lee, H. W.; Lee, S. M.; Jae, J.; Park, Y. K. Overview of the Recent Advances in
624 Lignocellulose Liquefaction for Producing Biofuels, Bio-Based Materials and Chemicals. *Bioresour.*
625 *Technol.* **2019**, *279*, 373–384. <https://doi.org/10.1016/j.biortech.2019.01.055>.
- 626 (3) Nguyen, T. D. H.; Maschietti, M.; Belkheiri, T.; Åmand, L. E.; Theliander, H.; Wamling, L.; Olausson,
627 L.; Andersson, S. I. Catalytic Depolymerisation and Conversion of Kraft Lignin into Liquid Products
628 Using Near-Critical Water. *J. Supercrit. Fluids* **2014**, *86*, 67–75.
629 <https://doi.org/10.1016/j.supflu.2013.11.022>.
- 630 (4) Pedersen, T. H.; Grigoras, I. F.; Hoffmann, J.; Toor, S. S.; Daraban, I. M.; Jensen, C. U.; Iversen, S. B.;
631 Madsen, R. B.; Glasius, M.; Arturi, K. R.; et al. Continuous Hydrothermal Co-Liquefaction of Aspen
632 Wood and Glycerol with Water Phase Recirculation. *Appl. Energy* **2016**, *162*, 1034–1041.
633 <https://doi.org/10.1016/j.apenergy.2015.10.165>.
- 634 (5) Jarvis, J. M.; Billing, J. M.; Hallen, R. T.; Schmidt, A. J.; Schaub, T. M. Hydrothermal Liquefaction
635 Biocrude Compositions Compared to Petroleum Crude and Shale Oil. *Energy and Fuels* **2017**, *31*, 2896–
636 2906. <https://doi.org/10.1021/acs.energyfuels.6b03022>.
- 637 (6) Jensen, C. U.; Rodriguez Guerrero, J. K.; Karatzos, S.; Olofsson, G.; Iversen, S. B. Fundamentals of
638 Hydrofaction™: Renewable Crude Oil from Woody Biomass. *Biomass Convers. Biorefinery* **2017**, *7*,
639 495–509. <https://doi.org/10.1007/s13399-017-0248-8>.
- 640 (7) Jensen, C. U.; Rosendahl, L. A.; Olofsson, G. Impact of Nitrogenous Alkaline Agent on Continuous HTL
641 of Lignocellulosic Biomass and Biocrude Upgrading. *Fuel Process. Technol.* **2017**, *159*, 376–385.
642 <https://doi.org/10.1016/j.fuproc.2016.12.022>.

- 643 (8) Cao, L.; Zhang, C.; Chen, H.; Tsang, D. C. W.; Luo, G.; Zhang, S.; Chen, J. Hydrothermal Liquefaction
644 of Agricultural and Forestry Wastes: State-of-the-Art Review and Future Prospects. *Bioresour. Technol.*
645 **2017**, *245*, 1184–1193. <https://doi.org/10.1016/j.biortech.2017.08.196>.
- 646 (9) Ong, B. H. Y.; Walmsley, T. G.; Atkins, M. J.; Walmsley, M. R. W. Hydrothermal Liquefaction of
647 Radiata Pine with Kraft Black Liquor for Integrated Biofuel Production. *J. Clean. Prod.* **2018**, *199*, 737–
648 750. <https://doi.org/10.1016/j.jclepro.2018.07.218>.
- 649 (10) Jarvis, J. M.; Albrecht, K. O.; Billing, J. M.; Schmidt, A. J.; Hallen, R. T.; Schaub, T. M. Assessment of
650 Hydrotreatment for Hydrothermal Liquefaction Biocrudes from Sewage Sludge, Microalgae, and Pine
651 Feedstocks. *Energy and Fuels* **2018**, *32*, 8483–8493. <https://doi.org/10.1021/acs.energyfuels.8b01445>.
- 652 (11) Belkheiri, T.; Andersson, S. I.; Mattsson, C.; Olausson, L.; Thelander, H.; Vamling, L. Hydrothermal
653 Liquefaction of Kraft Lignin in Sub-Critical Water: The Influence of the Sodium and Potassium Fraction.
654 *Biomass Convers. Biorefinery* **2018**, *8*, 585–595. <https://doi.org/10.1007/s13399-018-0307-9>.
- 655 (12) Anastasakis, K.; Biller, P.; Madsen, R. B.; Glasius, M.; Johannsen, I. Continuous Hydrothermal
656 Liquefaction of Biomass in a Novel Pilot Plant with Heat Recovery and Hydraulic Oscillation. *Energies*
657 **2018**, *11*, 1–23. <https://doi.org/10.3390/en11102695>.
- 658 (13) Sintamarean, I. M.; Grigoras, I. F.; Jensen, C. U.; Toor, S. S.; Pedersen, T. H.; Rosendahl, L. A. Two-
659 Stage Alkaline Hydrothermal Liquefaction of Wood to Biocrude in a Continuous Bench-Scale System.
660 *Biomass Convers. Biorefinery* **2017**, *7*, 425–435. <https://doi.org/10.1007/s13399-017-0247-9>.
- 661 (14) Arturi, K. R.; Strandgaard, M.; Nielsen, R. P.; Søgaard, E. G.; Maschietti, M. Hydrothermal Liquefaction
662 of Lignin in Near-Critical Water in a New Batch Reactor: Influence of Phenol and Temperature. *J.*
663 *Supercrit. Fluids* **2017**, *123*, 28–39. <https://doi.org/10.1016/j.supflu.2016.12.015>.
- 664 (15) Nguyen Lyckeskog, H.; Mattsson, C.; Åmand, L. E.; Olausson, L.; Andersson, S. I.; Vamling, L.;

- 665 Theliander, H. Storage Stability of Bio-Oils Derived from the Catalytic Conversion of Softwood Kraft
666 Lignin in Subcritical Water. *Energy and Fuels* **2016**, *30*, 3097–3106.
667 <https://doi.org/10.1021/acs.energyfuels.6b00087>.
- 668 (16) Lyckeskog, H. N.; Mattsson, C.; Olausson, L.; Andersson, S. I.; Vamling, L.; Theliander, H. Thermal
669 Stability of Low and High Mw Fractions of Bio-Oil Derived from Lignin Conversion in Subcritical
670 Water. *Biomass Convers. Biorefinery* **2017**, *7*, 401–414. <https://doi.org/10.1007/s13399-016-0228-4>.
- 671 (17) Hoffmann, J.; Jensen, C. U.; Rosendahl, L. A. Co-Processing Potential of HTL Bio-Crude at Petroleum
672 Refineries – Part 1: Fractional Distillation and Characterization. *Fuel* **2016**, *165*, 526–535.
673 <https://doi.org/10.1016/j.fuel.2015.10.094>.
- 674 (18) Pedersen, T. H.; Jensen, C. U.; Sandström, L.; Rosendahl, L. A. Full Characterization of Compounds
675 Obtained from Fractional Distillation and Upgrading of a HTL Biocrude. *Appl. Energy* **2017**, *202*, 408–
676 419. <https://doi.org/10.1016/j.apenergy.2017.05.167>.
- 677 (19) Ramirez, J. A.; Brown, R. J.; Rainey, T. J. A Review of Hydrothermal Liquefaction Bio-Crude Properties
678 and Prospects for Upgrading to Transportation Fuels. *Energies* **2015**, *8*, 6765–6794.
679 <https://doi.org/10.3390/en8076765>.
- 680 (20) Haarlemmer, G.; Guizani, C.; Anouti, S.; Déniel, M.; Roubaud, A.; Valin, S. Analysis and Comparison of
681 Bio-Oils Obtained by Hydrothermal Liquefaction and Fast Pyrolysis of Beech Wood. *Fuel* **2016**, *174*,
682 180–188. <https://doi.org/10.1016/j.fuel.2016.01.082>.
- 683 (21) Déniel, M.; Haarlemmer, G.; Roubaud, A.; Weiss-Hortala, E.; Fages, J. Optimisation of Bio-Oil
684 Production by Hydrothermal Liquefaction of Agro-Industrial Residues: Blackcurrant Pomace (*Ribes*
685 *Nigrum* L.) as an Example. *Biomass and Bioenergy* **2016**, *95*, 273–285.
686 <https://doi.org/10.1016/j.biombioe.2016.10.012>.

- 687 (22) Montesantos, N.; Pedersen, T. H.; Nielsen, R. P.; Rosendahl, L.; Maschietti, M. Supercritical Carbon
688 Dioxide Fractionation of Bio-Crude Produced by Hydrothermal Liquefaction of Pinewood. *J. Supercrit.*
689 *Fluids* **2019**, *149*, 97–109. [https://doi.org/https://doi.org/10.1016/j.supflu.2019.04.001](https://doi.org/10.1016/j.supflu.2019.04.001).
- 690 (23) Elliott, D. C. Historical Developments in Hydroprocessing Bio-Oils. *Energy and Fuels* **2007**, *21*, 1792–
691 1815. <https://doi.org/10.1021/ef070044u>.
- 692 (24) Leijenhorst, E. J.; Wolters, W.; Van De Beld, L.; Prins, W. Inorganic Element Transfer from Biomass to
693 Fast Pyrolysis Oil: Review and Experiments. *Fuel Process. Technol.* **2016**, *149*, 96–111.
694 <https://doi.org/10.1016/j.fuproc.2016.03.026>.
- 695 (25) Furimsky, E.; Massoth, F. E. Deactivation of Hydroprocessing Catalysts. *Catal. Today* **1999**, *52*, 381–
696 495. [https://doi.org/10.1016/S0920-5861\(99\)00096-6](https://doi.org/10.1016/S0920-5861(99)00096-6).
- 697 (26) Eijssbouts, S.; Battiston, A. A.; van Leerdam, G. C. Life Cycle of Hydroprocessing Catalysts and Total
698 Catalyst Management. *Catal. Today* **2008**, *130*, 361–373. <https://doi.org/10.1016/j.cattod.2007.10.112>.
- 699 (27) ASTM International. ASTM D1655-19a, Standard Specification for Aviation Turbine Fuels. West
700 Conshohocken, PA 2019. <https://doi.org/10.1520/D1655-19A>.
- 701 (28) European Committee for Standardization. EN590:2013+A1 Automotive Fuels -Diesel -Requirements and
702 Test Methods. 2017.
- 703 (29) ISO 8217:2017, Petroleum Products — Fuels (Class F) — Specifications of Marine Fuels. 2017.
- 704 (30) Brunner, G. Counter-Current Separations. *J. Supercrit. Fluids* **2009**, *47*, 574–582.
705 <https://doi.org/10.1016/j.supflu.2008.09.022>.
- 706 (31) Nielsen, R. P.; Valsecchi, R.; Strandgaard, M.; Maschietti, M. Experimental Study on Fluid Phase
707 Equilibria of Hydroxyl-Terminated Perfluoropolyether Oligomers and Supercritical Carbon Dioxide. *J.*
708 *Supercrit. Fluids* **2015**, *101*, 124–130. <https://doi.org/10.1016/j.supflu.2015.03.011>.

- 709 (32) Riha, V.; Brunner, G. Separation of Fish Oil Ethyl Esters with Supercritical Carbon Dioxide. *J. Supercrit.*
710 *Fluids* **2000**, *17*, 55–64. [https://doi.org/10.1016/S0896-8446\(99\)00038-8](https://doi.org/10.1016/S0896-8446(99)00038-8).
- 711 (33) Gironi, F.; Maschietti, M. Separation of Fish Oils Ethyl Esters by Means of Supercritical Carbon
712 Dioxide: Thermodynamic Analysis and Process Modelling. *Chem. Eng. Sci.* **2006**, *61*, 5114–5126.
713 <https://doi.org/10.1016/j.ces.2006.03.041>.
- 714 (34) Dunford, N. T.; Teel, J. A.; King, J. W. A Continuous Countercurrent Supercritical Fluid Deacidification
715 Process for Phytosterol Ester Fortification in Rice Bran Oil. *Food Res. Int.* **2003**, *36*, 175–181.
716 [https://doi.org/10.1016/S0963-9969\(02\)00134-5](https://doi.org/10.1016/S0963-9969(02)00134-5).
- 717 (35) Eisenmenger, M.; Dunford, N. T.; Eller, F.; Taylor, S.; Martinez, J. Pilot-Scale Supercritical Carbon
718 Dioxide Extraction and Fractionation of Wheat Germ Oil. *JAACS, J. Am. Oil Chem. Soc.* **2006**, *83*, 863–
719 868. <https://doi.org/10.1007/s11746-006-5038-6>.
- 720 (36) Vázquez, L.; Torres, C. F.; Fornari, T.; Señoráns, F. J.; Reglero, G. Recovery of Squalene from
721 Vegetable Oil Sources Using Countercurrent Supercritical Carbon Dioxide Extraction. *J. Supercrit.*
722 *Fluids* **2007**, *40*, 59–66. <https://doi.org/10.1016/j.supflu.2006.04.012>.
- 723 (37) Montesantos, N.; Pedersen, T. H.; Nielsen, R. P.; Rosendahl, L. A.; Maschietti, M. High-Temperature
724 Extraction of Lignocellulosic Bio-Crude by Supercritical Carbon Dioxide. *Chem. Eng. Trans.* **2019**, *74*,
725 799–804. <https://doi.org/10.3303/CET1974134>.
- 726 (38) Jensen, C. U. PIUS – Hydrofaction™ Platform with Integrated Upgrading Step, PhD Thesis, Aalborg
727 University, 2018.
- 728 (39) Patel, R. N.; Bandyopadhyay, S.; Ganesh, A. Extraction of Cardanol and Phenol from Bio-Oils Obtained
729 through Vacuum Pyrolysis of Biomass Using Supercritical Fluid Extraction. *Energy* **2011**, *36*, 1535–
730 1542. <https://doi.org/10.1016/j.energy.2011.01.009>.

- 731 (40) Feng, Y.; Meier, D. Supercritical Carbon Dioxide Extraction of Fast Pyrolysis Oil from Softwood. *J.*
732 *Supercrit. Fluids* **2017**, *128*, 6–17. <https://doi.org/10.1016/j.supflu.2017.04.010>.
- 733 (41) Feng, Y.; Meier, D. Extraction of Value-Added Chemicals from Pyrolysis Liquids with Supercritical
734 Carbon Dioxide. *J. Anal. Appl. Pyrolysis* **2015**, *113*, 174–185. <https://doi.org/10.1016/j.jaap.2014.12.009>.
- 735 (42) ASTM International. *ASTM D664-17a, Standard Test Method for Acid Number of Petroleum Products by*
736 *Potentiometric Titration*; West Conshohocken, PA, 2017. <https://doi.org/10.1520/D0664-17A>.
- 737 (43) Lemmon, E. W.; McLinden, M. O.; Friend, D. G. Thermophysical Properties of Fluid Systems. In *NIST*
738 *Chemistry WebBook, NIST Standard Reference Database Number 69*; Linstrom, P. J., Mallard, W. G.,
739 Eds.; National Institute of Standards and Technology: Gaithersburg MD, 20899.
740 <https://doi.org/https://doi.org/10.18434/T4D303>.
- 741 (44) Oasmaa, A.; Van De Beld, B.; Saari, P.; Elliott, D. C.; Solantausta, Y. Norms, Standards, and Legislation
742 for Fast Pyrolysis Bio-Oils from Lignocellulosic Biomass. *Energy and Fuels* **2015**, *29*, 2471–2484.
743 <https://doi.org/10.1021/acs.energyfuels.5b00026>.
- 744 (45) Madsen, R. B.; Bernberg, R. Z. K.; Biller, P.; Becker, J.; Iversen, B. B.; Glasius, M. Hydrothermal Co-
745 Liquefaction of Biomasses – Quantitative Analysis of Bio-Crude and Aqueous Phase Composition.
746 *Sustain. Energy Fuels* **2017**, *1*, 789–805. <https://doi.org/10.1039/C7SE00104E>.
- 747 (46) Rowell, R.; Pettersen, R.; Tshabalala, M. Cell Wall Chemistry. In *Handbook of Wood Chemistry and*
748 *Wood Composites, Second Edition*; Rowell, R. M., Ed.; CRC Press, 2012; pp 33–72.
749 <https://doi.org/10.1201/b12487-5>.
- 750 (47) Vassilev, S. V.; Baxter, D.; Andersen, L. K.; Vassileva, C. G.; Morgan, T. J. An Overview of the Organic
751 and Inorganic Phase Composition of Biomass. *Fuel* **2012**, *94*, 1–33.
752 <https://doi.org/10.1016/j.fuel.2011.09.030>.

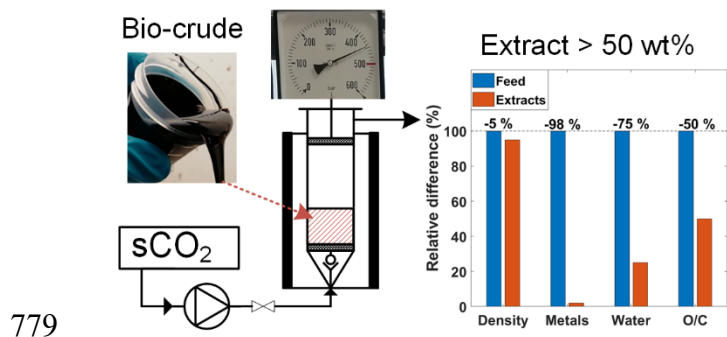
- 753 (48) Nguyen, T. D. H.; Maschietti, M.; Åmand, L. E.; Vamling, L.; Olausson, L.; Andersson, S. I.; Theliander,
754 H. The Effect of Temperature on the Catalytic Conversion of Kraft Lignin Using Near-Critical Water.
755 *Bioresour. Technol.* **2014**, *170*, 196–203. <https://doi.org/10.1016/j.biortech.2014.06.051>.
- 756 (49) Standley, L. J.; Simoneit, B. R. T. Resin Diterpenoids as Tracers for Biomass Combustion Aerosols. *J.*
757 *Atmos. Chem.* **1994**, *18*, 1–15. <https://doi.org/10.1007/BF00694371>.
- 758 (50) Carpy, A.; Marchand-Geneste, N. Molecular Characterization of Retene Derivatives Obtained by
759 Thermal Treatment of Abietane Skeleton Diterpenoids. *J. Mol. Struct. THEOCHEM* **2003**, *635*, 45–53.
760 [https://doi.org/10.1016/S0166-1280\(03\)00400-7](https://doi.org/10.1016/S0166-1280(03)00400-7).
- 761 (51) Madsen, R. B.; Zhang, H.; Biller, P.; Goldstein, A. H.; Glasius, M. Characterizing Semivolatile Organic
762 Compounds of Biocrude from Hydrothermal Liquefaction of Biomass. *Energy and Fuels* **2017**, *31*, 4122–
763 4134. <https://doi.org/10.1021/acs.energyfuels.7b00160>.
- 764 (52) McHugh, M. A.; Krukonis, V. J. Phase Diagrams for Supercritical Fluid–Solute Mixtures. In
765 *Supercritical Fluid Extraction*; Brenner, H., Ed.; Elsevier, 1994; pp 27–84. [https://doi.org/10.1016/B978-](https://doi.org/10.1016/B978-0-08-051817-6.50006-0)
766 [0-08-051817-6.50006-0](https://doi.org/10.1016/B978-0-08-051817-6.50006-0).
- 767 (53) Kokayeff, P.; Zink, S.; Roxas, P. Hydrotreating in Petroleum Processing. In *Handbook of Petroleum*
768 *Processing*; Treese, S. A., Pujadó, P. R., Jones, D. S. J., Eds.; Springer International Publishing, 1995; pp
769 363–434.
- 770 (54) Mortensen, P. M.; Grunwaldt, J. D.; Jensen, P. A.; Knudsen, K. G.; Jensen, A. D. A Review of Catalytic
771 Upgrading of Bio-Oil to Engine Fuels. *Appl. Catal. A Gen.* **2011**, *407*, 1–19.
772 <https://doi.org/10.1016/j.apcata.2011.08.046>.
- 773 (55) Bjelić, S.; Yu, J.; Iversen, B. B.; Glasius, M.; Biller, P. Detailed Investigation into the Asphaltene
774 Fraction of Hydrothermal Liquefaction Derived Bio-Crude and Hydrotreated Bio-Crudes. *Energy and*

775 *Fuels* **2018**, 32, 3579–3587. <https://doi.org/10.1021/acs.energyfuels.7b04119>.

776

777

Accepted author manuscript



Accepted author manuscript